Appl Phys B (2011) 104:975–982
DOI 10.1007/s00340-011-4612-2

Applied Physics B
Lasers and Optics

Comparison of indigenously developed micro pulse polarization lidar with EZ lidar profiles

R. Maurya · P.K. Dubey · D.K. Shukla · A. Kumar · B.C. Arya · S.L. Jain

Received: 9 December 2010 / Revised version: 9 May 2011 / Published online: 12 July 2011

Abstract A Micro Pulse Polarization LIDAR (MPPL) has been designed and developed for aerosol and cloud studies at National Physical Laboratory, New Delhi, India (28° 35′ N, 77° 12′E) using a low-energy pico-second pulsed Nd:YAG laser at 532 nm and single PMT detector. This has been used for detecting depolarization characteristics with back-scatter coefficient of atmospheric aerosols and clouds. The back-scattered signals are detected at the emitted wavelength with co-polarization and cross-polarization discrimination with a mirror on stepper motor for aerosols and cloud. Data are obtained by MPPL and are inter-compared with a well-established commercial Leosphere made EZ LIDAR, industry standard at the same site and time, and the results are found to be in good agreement. In the present communication the back-scattered coefficient, aerosols optical depth, depolarization ratio etc. obtained using MPPL & EZ LIDAR are discussed in detail.

1 Introduction

Characterization of the atmosphere requires a number of meteorological data like temperature, pressure, humidity and wind direction etc. To understand the atmospheric processes, atmospheric aerosols are also being considered in meteorological studies for they are required in climate models. It is thought that an aerosol may be involved in a feedback to global warming. It is certainly important in the earth's radiation budget. There are also many concerns about the effects of aerosol on human health. Scattering and absorption characteristics of aerosols have a variety of implications in the troposphere (i.e. seeding troposphere clouds and formation of haze and fog, thereby re-distribution of the incoming solar flux and the infrared terrestrial emission), and altering the radiation balance of system of the earth [1]. A large uncertainty exists in radiation forcing due to aerosols; therefore, measurement of vertical distribution of aerosols is essential to reduce the uncertainties due to its distribution in radiative forcing.

LIDAR is a promising tool and plays an important role in remote sensing of vertical profile of aerosols back-scatter and extinction coefficient. In particular, the use of polarization LIDAR permits the measurement of aerosol extinction and back-scatter with aerosols structures distribution w.r.t. height. The LIDAR signal is the superposition of scattering that is due to molecules and scattering that is due to particles that are greater than the typical dimensions of atmospheric molecules. Molecular backscattering follows Rayleigh theory, in this case changes in polarization are due to the polarizability of molecules. Scattering processes on aerosols must be treated by means of Mie theory if particles are spherical. From Mie theory, the polarization of incident light is conserved after back-scattering, whereas back-scattering on solid particles can change the polarization direction. If a laser beam is emitted with a definite polarization, the presence of polarized light in the perpendicular component denotes the presence of back-scattering from non-spherical particles. Hence, polarized back-scattering (parallel to the laser polarization) is considered and depolarization is used to refer to the perpendicular component of polarized back-scattered light.

Polarization LIDAR is an active remote sensing instrument that emits low-energy laser pulses toward the at-

R. Maurya (✉) · P.K. Dubey · D.K. Shukla · A. Kumar · B.C. Arya · S.L. Jain
Radio and Atmospheric Sciences Division, National Physical Laboratory, Dr. K.S. Krishnan Marg, New Delhi 110012, India
e-mail: mauryarenu@yahoo.com
Fax: +91-11-45608584

mosphere or target and measures the back-scattered signal [2]. Polarization LIDAR is being widely used to monitor meteorological parameters, atmospheric constituents and their structures [3, 4]. The basic polarization LIDAR application involves the transmission of a linearly polarized laser pulse and the detection of the orthogonal and parallel polarization components of the back-scattered light via a beam splitter. The ratio of these two signals is referred to as the depolarization ratio [3, 5]. The depolarization ratio provides the information about the particle shape, whether the particles are spherical or non-spherical [4].

In this paper the vertical profiles of the aerosol backscatter characteristics at 532 nm have been determined through an iterative procedure based on the assumption of a constant value for the extinction-to-back-scattering ratio within the nocturnal boundary layer using indigenously developed Micro Pulse Polarization LIDAR (MPPL) at National Physical Laboratory (NPL), New Delhi, India. The MPPL system provides vertical profiling of aerosols and clouds with high temporal and spatial resolution, which makes it possible to observe the atmosphere at ambient conditions and permit a clear separation of optical properties of boundary layer particles. To verify the indigenous LIDAR data, a well-established Leosphere made EZ LIDAR also was run in parallel on the same time along with indigenously developed MPPL.

Polarization LIDARs are being widely used for the study of aerosols and clouds because of their ability to discriminate not only ice from water but also spherical particles from particles of irregular shape [6–8]. Because the cross-polarized component can only arise from the multiple scattering processes, observation of this component can provide a direct measure of the multiple scattering taking place in the medium [9–11]. Murayama et al. [12] had also demonstrated the application of depolarization LIDAR for the measurements of aerosols composition and found aerosols depolarization is caused by dust or crystallized sea salt. Dust, biomass burning and sea salt are possible sources of non-spherical particles. We present some typical results obtained by aforesaid LIDARs during cloudy/drizzle and clear atmosphere at NPL, New Delhi (28° 35′ N, 77° 12′ E), India.

2 Experimental set-up and analysis

A portable MPL system was indigenously designed and developed at NPL, New Delhi, for the study of aerosols and clouds and their depolarization ratio measurements. The LIDAR system uses a 532 nm, Nd:YAG, diode pumped solid state pulsed laser having 900 pico-second pulse width and 4 μJ pulse power. The MPPL is capable to acquire continuous back-scattered data without user interaction. The laser pulse is transmitted into the atmosphere through a 8× optical beam expander. A co-axial receiver transmitter assembly is used to have the overlapping of laser beam and telescope field of view (FOV) at lower altitude. A Cassegrainian telescope is used to reduce the overall length of the receiver. The back-scattered light received by telescope is passed through the orifice to limit the field of view of the receiver. The light is then passed through a collimator, interference filter (3 nm BW), 532 nm Fabry-Pérot etalon and polarization beam splitter. Along with the conventional receiver optics a high gain photo multiplier tube (PMT) is used to receive the back-scattered photons. As the transmitted laser pulse energy is low, a photon counting technique is employed at high repetition rate (7.5 kHz) to achieve a wide dynamic range of the measured signal.

To minimize the error in depolarization ratio measurements due to the difference in the electronic gains of the two channels, the dual polarization detection system using single PMT has been successfully designed and is being used in MPPL system. The polarization beam splitter separates the received back-scattered signal into co-polarized (P) and cross-polarized (S) components. The two fixed mirrors are used to bring the cross-polarized signal beam on the reflecting surface of the Stepper Motor Controlled Rotating Mirror (SMCRM). This polarization selection mirror (SMCRM) has the reflecting front surface with absorbing coating at the back. This mirror is mounted on a micro stepping Stepper Motor. The stepping motor is driven in half step mode to achieve a step resolution of 0.9° [13, 14]. Software in visual basic using Graphical User Interface (GUI) has also been developed at NPL, New Delhi, for the control of the system. The specifications of the developed MPPL are given in Table 1.

The return signal, $P(Z)$, which is proportional to the received power from a scattering volume at a range Z, is given by

$$P(Z) = C \cdot E \cdot O(Z) \cdot Z^{-2} \cdot [\beta_a(Z) + \beta_m(Z)] \cdot T_a^2(Z) \cdot T_m^2(Z) + B_{bg} \quad (1)$$

where E is the output energy of the monitoring pulse which is proportional to the transmitted energy, C is the calibration constant of the instrument which includes losses in the transmitting and receiving optics and the effective receiver aperture. $O(Z)$ is the overlap correction as a function of range caused by field of view conflicts in the transmitter is equal to 1. $\beta_a(Z)$ and $\beta_m(Z)$ are the back-scattering coefficients of the aerosols and molecules at range Z. $T_{a,m}(Z)$, are the aerosols and molecular atmospheric transmittance, respectively. $T_{a,m}(Z) = \exp\cdot[-\int_0^Z \alpha_{a,m}(z)\,dz]$, with $\alpha_{a,m}(z)$ being the aerosols and molecular extinction coefficient, respectively. B_{bg} is the flux of photoelectrons due to background.

If we remove from (1) all instrument parameters except the calibration constant, and subtract the background contribution, it is possible to define the resulting signal from

Table 1 Specifications of MPPL system

Section	Parameter	Specification
Transmitter	Laser type	Diode pumped solid state Q-switched Nd:YAG laser
	Wavelength	532 nm
	Output pulse energy	4 μJoule
	Pulse duration	900 pS
	Pulse Repetition Rate	7.5 kHz
	Polarization	Linear
	Beam divergence (after beam expander)	150 μrad
Receiver	Telescope type	Schmidt Cassegranian
	Telescope diameter	20 cm
	Field of view (FOV)	<300 μrad
	Optical sensor	PMT, Hamamatsu: R647
Signal processing and electronics	Data acquisition technique	(single photon counting)
	Bin resolutions (selectable)	0.75 m, 6 m, 12 m, 24 m and 48 m
	Range (selectable)	1.5 km, 3 km, 6 km and 12 km
Control software	Software developed in visual basic under	Raw, background and dark count acquisition and Real time
	Windows XP environment	acquisition and display of back-scatter in one minute interval

the correction as the normalized correction back-scattering. Background correction and range correction could be done in software developed and corrected data are analyzed using Klett and Fernald solutions [15–18]. Applying the Fernald solution [18], the solution for aerosol back-scattering coefficient from LIDAR (1) after correction becomes

$$\beta_a(Z) = \frac{P(Z)Z^2 \exp\cdot[-2(S_1-S_2)\int_0^Z \beta_m(z)\,dz]}{CE - 2S_1\int_0^Z P(Z)Z^2 \exp\cdot[-2(S_1-S_2)\int_0^Z \beta_m(z')\,dz']\,dz} - \beta_m(Z) \quad (2)$$

where $S_1 = \alpha_a(Z)/\beta_a(Z)$, the extinction-to-back-scattering ratio for aerosols, and $S_2 = \alpha_m(Z)/\beta_m(Z) = 8\pi/3$ for the molecular scattering is a constant.

If a priori information can be used to specify the value of the aerosol and molecular scattering coefficient at a specific range Z_c, the LIDAR can be calibrated by solving (2) for CE in terms of these scattering properties and

$$\beta_a(z) + \beta_m(z) = \frac{X(Z)\exp\cdot[-2(S_1-S_2)\int_{Z_c}^Z \beta_m(z)\,dz]}{\frac{X(Z_c)}{\beta_a(Z_c)+\beta_m(Z_c)} - 2S_1\int_{Z_c}^Z X(z)\exp\cdot[-2(S_1-S_2)\int_{Z_c}^z \beta_m(z')\,dz']\,dz} \quad (3)$$

where $X(Z)$ is the range corrected signal $P(Z)\cdot Z^2$. LIDAR ratio, $S_1 = 50$ sr is assumed according to Muller et al. [19]. US standard atmospheric model (1976) was used for molecular back-scatter and extinction coefficients. The total back-scattering coefficient at range Z is now expressed as a function of the scattering properties at the calibration range and those of the intervening atmosphere between the ranges Z_c and Z. Assuming the calibration range from 7 to 10 km, we can find the solution of the above equations. Since the signal-to-noise ratio (SNR) at these heights is poor, several bins are averaged to obtain the better SNR at calibration height.

Table 2 Key specifications of EZ LIDAR system

Parameters	Specifications
Laser	Tripled YAG 355 nm
Pulse Energy	16 mJ
Pulse Duration	5 ns
Pulse Repetition Rate	20 Hz
Performance	
Range Min/Max	0.5/20 km
Accumulation time (PBL)	10 s
Accumulation time (Cirrus)	30 s
Vertical resolution	1.5/15 m

The indigenously developed MPPL was running together with a commercial EZ LIDAR (Model ASL 450, Leosphere, France). The EZ LIDAR provides calibrated raw & range corrected data, back-scatter & extinction coefficient, back-scatter ratio, cloud layers (base, top if penetrable and multilayers if penetrable), PBL height (mixing layer), and optical depth. Validation of EZ LIDAR data has been made [20]. The specifications of EZ LIDAR are given in Table 2.

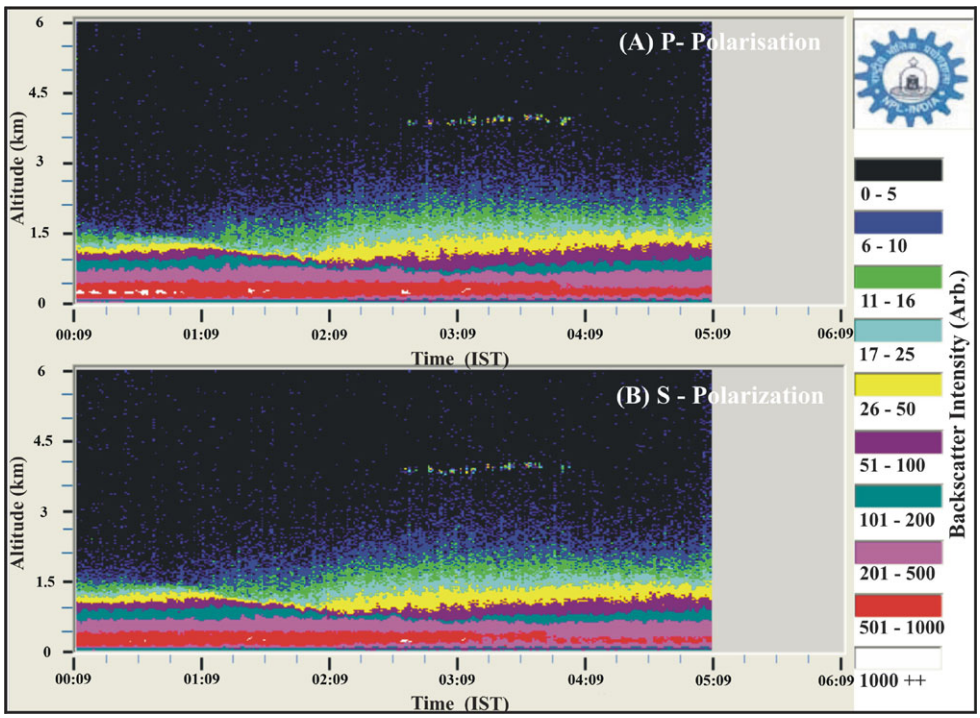

Fig. 1 Time evolution of the raw back-scattered energy observed in both (**A**) co-P (parallel) and (**B**) cross-S (perpendicular) polarization channels of the MPPL in the night of 21st–22nd April, 2010 from 00:30 to 05:00 IST

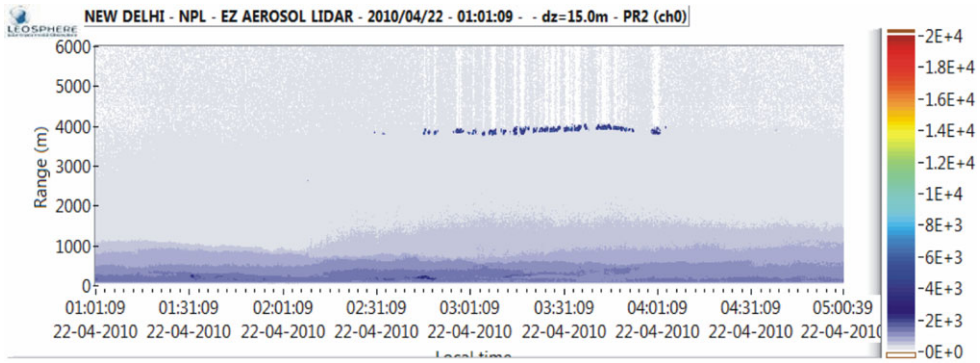

Fig. 2 Back-scattered energy observed with EZ LIDAR based on 355 nm of Nd:YAG laser in the night of 21st–22nd April, 2010 from 01:00 to 05:00 IST

3 Results and discussion

3.1 Observations

Figures 1, 3 and 5 show the P and S polarization signal from MPPL received in the night of 21st–22nd April and 30th April–01st May, 2010. On 22nd April 2010, a cloud was observed with the help of MPPL system during 2.30 to 4.15 IST after mid night at New Delhi as shown in Fig. 1. The signature of the cloud is also observed by EZ LIDAR at the same time and height as depicted in Fig. 2. The inter-comparison of data from the indigenously developed MPPL is in good agreement with that of the EZ LIDAR measurements, which demonstrate the notable performance of MPPL system. A dust storm and a trace of rain could be observed in the night of 30th April—01st May, 2010. Figures 3 and 5 depict the back-scatter signal from MPPL recorded on 30th April–01st May, 2010. In the night of 30th April–01st May, 2010, an event of rain could be observed about 20.00 IST, but due to rain MPPL system had to shut down. Again an event of rain could be found during 22:50 to 23:05 IST. We start observing the formation of another layer of cloud after 00:10 IST at varying heights from 4.0 to 6.0 km above the ground. The modification in meteorological parameters is due to the complex terrain of the experimental site, it also plays an important role in the generation, transformation, transport and removal of aerosols and cloud properties in the atmosphere. Also seen are the fragmented cloud structures at altitudes ranging from 3.0 to 7.0 km. In order to examine MPPL data, we have also operated EZ LIDAR at the same time as shown in Figs. 4 and 6. Both LIDARs show similar behavior in the boundary layer processes and structural changes in the clouds as can be clearly seen in Figs. 1 and 6.

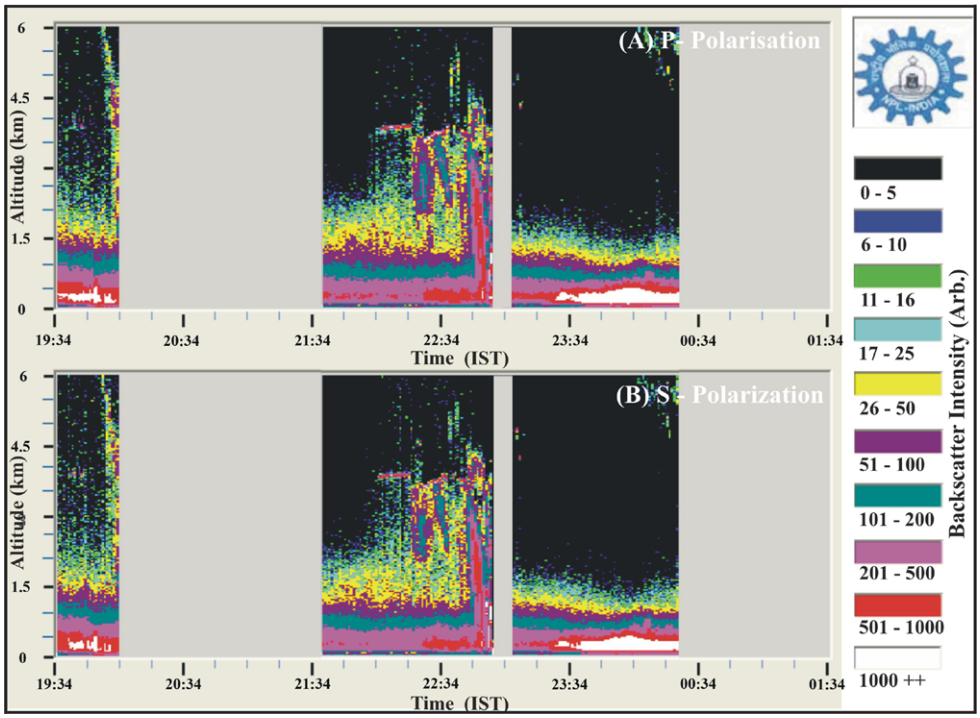

Fig. 3 Time evolution of the raw back-scattered energy observed in both (**A**) co-P (parallel) and (**B**) cross-S (perpendicular) polarization channels of the MPPL in the night of 30th April–01st May, 2010 from 19:30 to 00:30 IST

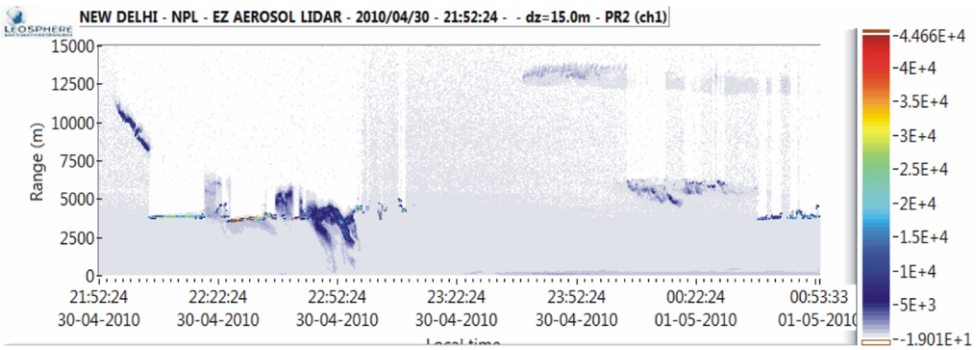

Fig. 4 Back-scattered energy observed with EZ LIDAR based on 355 nm of Nd:YAG laser in the night of 30th April–01st May, 2010 from 22:00 to 00:30 IST

3.2 Back-scatter coefficient

Figure 7 shows the aerosol back-scatter coefficient from the MPPL measurement taken at New Delhi in the night of 30th April–01st May, 2010.

The example in Fig. 7 shows strongly absorbing anthropogenic pollution advected for the Indian subcontinent to the LIDAR site. As can be seen in Fig. 7 aerosols and clouds were present over New Delhi in the night of 30th April–01st May, 2010 at different time. Figure 8 shows consecutive aerosols optical depth of the data shown in Fig. 7 calculated with the extinction profile. Descending of the cloud w.r.t. time and onset of the rain at an optimum height can be observed here.

3.3 Depolarization

Figures 9 and 10 show the profiles of depolarization ratio for cirrus clouds and aerosols over New Delhi, India, which helps to identify the cloud phase (water or ice or both) and isotropy/anisotropy nature of aerosol particles in the experimental region. The plot of depolarization ratio reveals low values of depolarization ratio suggesting that the clouds contain liquid droplets in the study region. The value of the depolarization ratio of spherical particles such as liquid droplet is tending to zero for back-scattering, based on the Mie scattering theory; enhancement of the depolarization ratio can arise from scattering by non-spherical particles such as solid particles or by multiple scattering [19]. The depolarization detection capability of the technique has been already presented by Dubey et al. [13]. In the lower altitude the higher value of depolarization ratio reveals dust and biomass burning particles that are possible sources of non-spherical particles. Due to a strong dust storm and then cloud formation in the night of 30th April–01st May, 2010 particles having higher depolarization ratio are distributed at lower altitude and particles having smaller depolarization ratio lie at higher

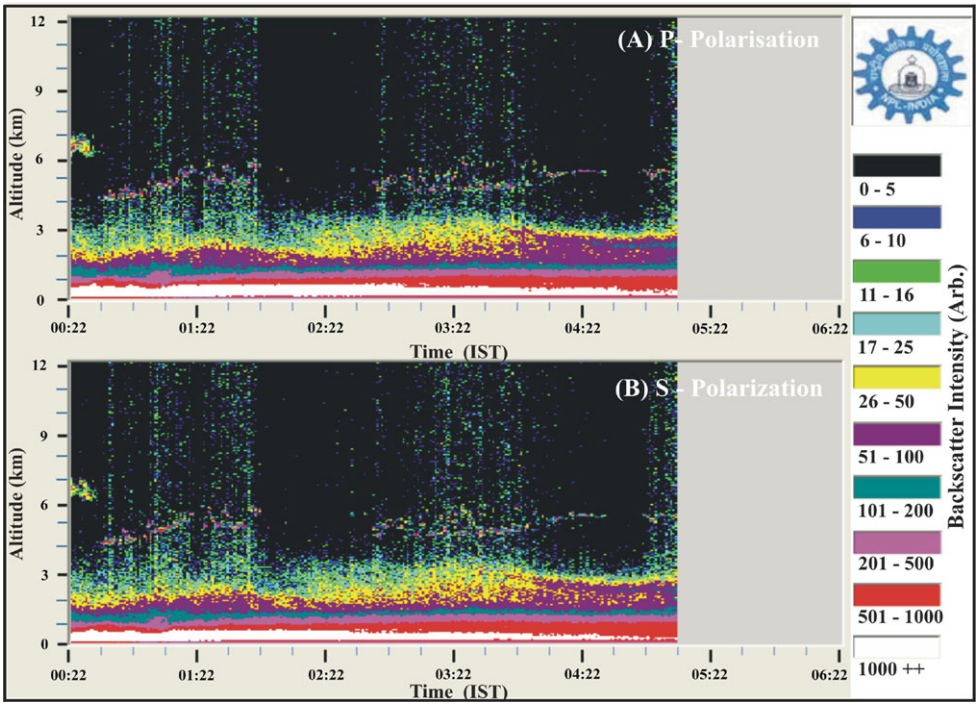

Fig. 5 Time evolution of the raw back-scattered energy observed in both (**A**) co-P (parallel) and (**B**) cross-S (perpendicular) polarization channels of the MPPL in the night of 30th April–01st May, 2010 from 00:30 to 05:00 IST

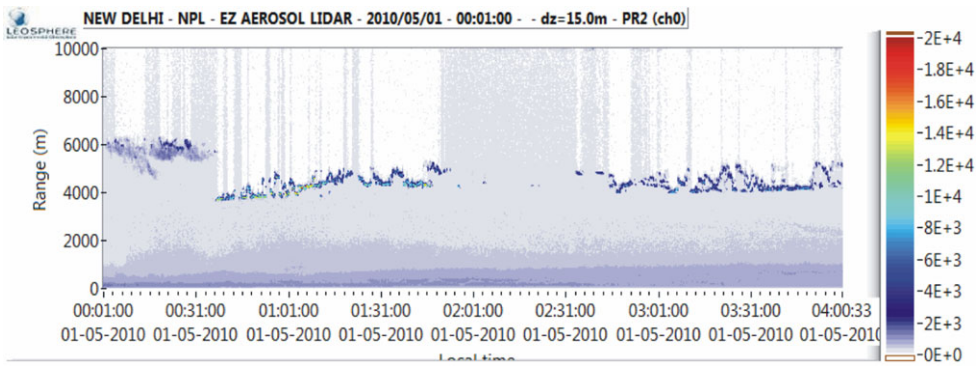

Fig. 6 Back-scattered energy observed with EZ LIDAR based on 355 nm of Nd:YAG laser in the night of 30th April–01st May, 2010 from 00:00 to 04:00 IST

altitude. Asian mineral dust had been identified to contain significant amounts of calcium [21], thus Ca^{2+} is one of the species that is most enhanced in dust storm events [22–24].

Biomass burning in Asia is an important contributor with about $22 \pm 8\%$ to light scattering in outflow from East Asia. Therefore, biomass burning might exhibit significant depolarization if there is enough concentration. Because of the observed values of depolarization contributions are reflected from all kinds of aerosols, and the higher value of depolarization ratio implies that the percentage of non-spherical particle is higher. The observed non-spherical particles are not easy to be deliquescent, the inhomogeneous vertical distribution of depolarization ratio may be caused by hygroscopic property of the aerosol, which makes the scattering cross section of spherical particles increase under higher relative humidity and hence we have subsequent reduction in the depolarization ratio. Inside the cloud, enormous cloud back-scatter did not as expected to reduce the depolarization ratio to zero that might be caused by multiscattering effect.

4 Conclusions

The indigenously developed MPPL and EZ LIDAR were used at NPL New Delhi to get back-scatter coefficient, extinction coefficient and aerosol optical depth profile. Inter-comparison of measurements shows that indigenously developed MPPL and EZ LIDAR data sets are in good agreement; therefore, the MPPL system operating at second harmonic of Nd:YAG i.e. 532 nm using a single photomultiplier tube as a detector is capable to discriminate the P and S polarization channels with polarization beam splitter. With high temporal and vertical resolution of LIDAR, we found that it could distinguish the spherical and non-spherical particles with single PMT. It was also ob-

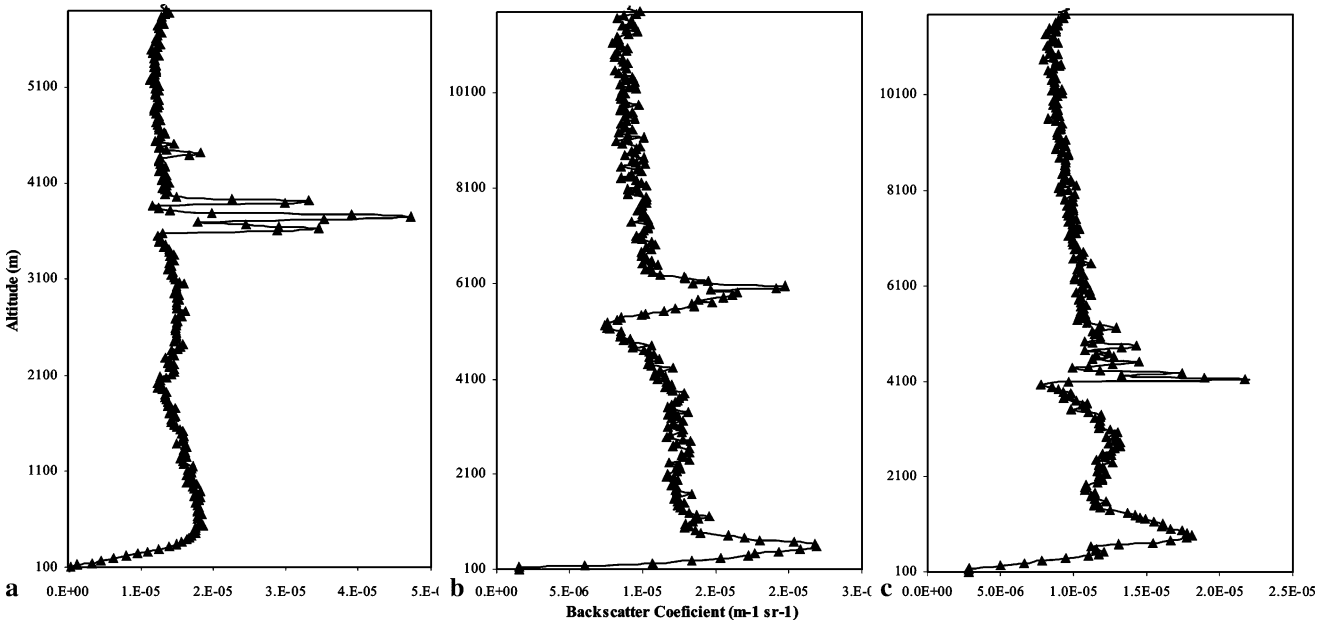

Fig. 7 Profiles of aerosols back-scatter coefficient (**a**) at 22.30 IST (**b**) at 00:15 IST and (**c**) at 3.15 IST, measured in the night of 30th April–01st May, 2010

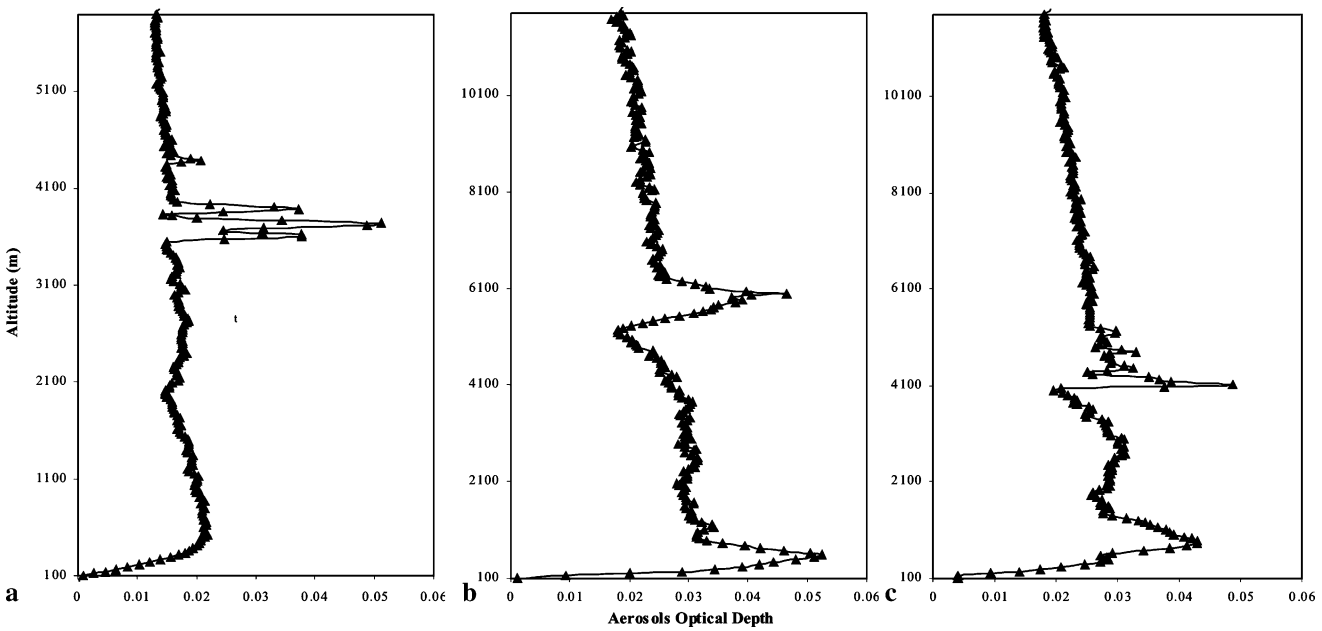

Fig. 8 Aerosols optical depth from integrated extinction coefficient (**a**) at 22.30 IST (**b**) at 00:15 IST and (**c**) at 03.15 IST, measured in the night of 30th April–01st May, 2010

served that clouds were coming down with time at some optimum height the rain standard. Therefore, LIDAR data may have the potential to provide the vertical information of aerosol which in turn could be used to ascertain aerosols radiative forcing, cloud dynamics and boundary layer studies.

Acknowledgements Authors are grateful to Director, NPL, New Delhi, for all support for carrying out the present studies. Thanks are also due for the financial support by the Council for Scientific and Industrial Research (CSIR), India, in the emeritus scientist scheme. We also express our gratitude to M/S Leosphere, France, to provide EZ LIDAR to operate at NPL, New Delhi, India.

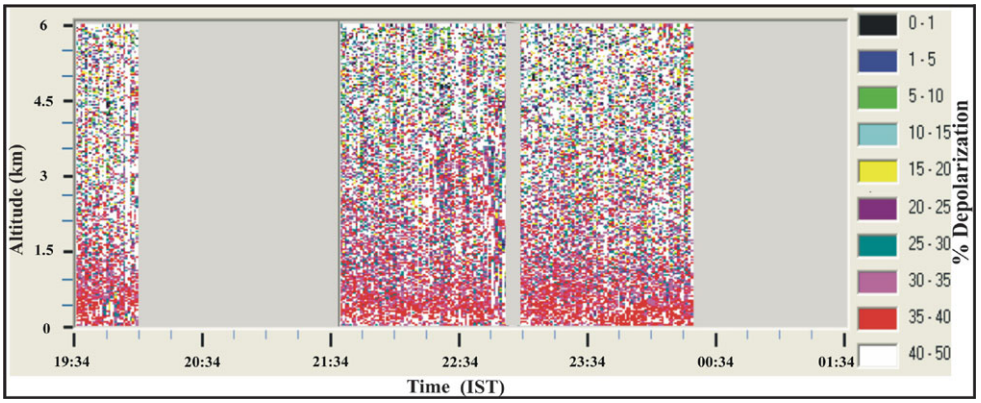

Fig. 9 Depolarization ratio of co-P (parallel) and cross-S (perpendicular) polarization signal of the MPPL profile monitored in the night of 30th April–01st May, 2010 during 19:34 to 00:20 IST

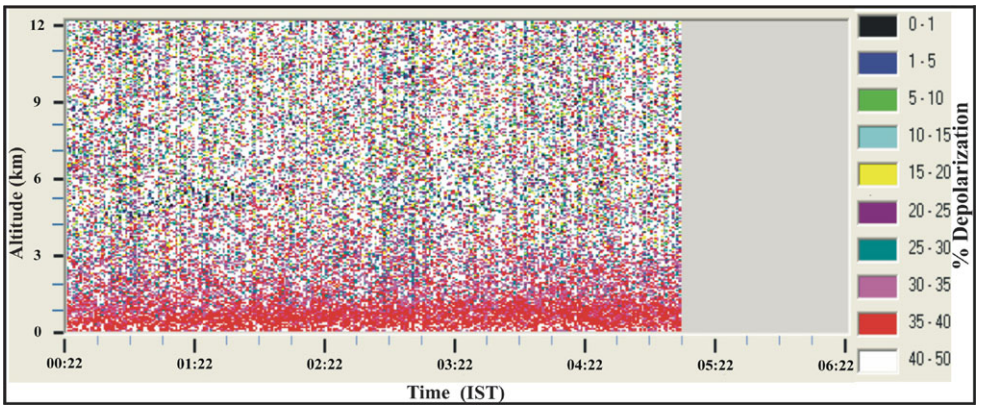

Fig. 10 Depolarization ratio of co-P (parallel) and cross-S (perpendicular) polarization signal of the MPPL profile monitored on the night of 30th April–01st May, 2010 during 00:22 to 05:10 IST

References

1. T. Fujii, T. Fukuchi, *Laser Remote Sensing*. Optical Engineering series, vol. 97 (CRC Press, Taylor & Francis Group, Boca Raton, London, 2005)
2. C.J. Flynn, A. Mendoza, Y. Zheng, S. Mathur, Opt. Express **15**(6), 2785 (2007)
3. U. Wandinger, in *Lidar*, ed. by C. Weitkamp (Springer, New York, 2005), p. 1
4. M. Shiobara, M. Yabuki, H. Kobeyashi, Phys. Chem. Earth **28**, 1205 (2003)
5. J. Biele, G. Beyerle, G. Baumgarten, Opt. Express **7**, 427 (2000)
6. C.W. Chiang, W.N. Chen, W.A. Liang, S.K. Das, J.B. Nee, Atmos. Environ. **41**, 4128 (2007)
7. S.R. Pal, A.I. Carswell, Appl. Opt. **12**, 1530 (1973)
8. K. Sassen, Bull. Am. Meteorol. Soc. **72**, 1848 (1991)
9. K. Sassen, in *Lidar*, ed. by C. Weitkamp (Springer, New York, 2005), p. 19
10. L.R. Bissonnette, G. Roy, F. Fabry, J. Atmos. Ocean. Technol. **18**, 1429 (2001)
11. L.R. Bissonnette, in *Lidar*, ed. by C. Weitkamp (Springer, New York, 2005), p. 43
12. T. Murayama, D. Müller, K. Wada, A. Shimizu, M. Sekiguchi, T. Tsukamoto, Geophys. Res. Lett. **31** (2004). doi:10.1029/2004GL021105
13. P.K. Dubey, S.L. Jain, B.C. Arya, P.S. Kulkarni, Rev. Sci. Instrum. **80**, 053111 (2009)
14. P.K. Dubey, S.L. Jain, B.C. Arya, P.S. Kulkarni, MAPAN, J. Metrol. Soc. India **25**, 63 (2010)
15. J.D. Klett, Appl. Opt. **20**, 211 (1981)
16. J.D. Klett, Appl. Opt. **24**, 1639 (1985)
17. F.G. Fernald, B.M. Herman, J.A. Reagan, J. Appl. Meteorol. **11**, 482 (1971)
18. F.G. Fernald, Appl. Opt. **23**, 653 (1984)
19. D. Muller, A. Ansmann, I. Mattis, M. Tesche, U. Wandinger, D. Althausen, G. Pisani, J. Geophys. Res. **112**, D16202 (2007). doi:10.1029/2006JD008292
20. S. Lolli, L. Sauvage, S. Loaec, M. Lardier, Opt. Pura Apl. **44**(1), 33–41 (2011)
21. A.R. Klekociuk, P.G. Brown, D.W. Pack, D.O. ReVelle, W.N. Edwards, R.E. Spalding, E. Tagliaferri, B.B. Yoo, J. Zagari, Nature **436**, 1132 (2005)
22. M. Nishikawa, Q. Hao, M. Morita, Glob. Environ. Res. **4**, 103 (2000)
23. C.C. Wang, C.T. Lee, S.C. Liu, J.P. Chen, Atmos. Oceanogr. Sci. **15**, 839 (2004)
24. J.C.H. Fung, A.K.H. Lau, J.S.L. Lam, Z. Yuan, J. Geophys. Res. **110**, D09105 (2005). doi:10.1029/2004JD005105